Original Article

Automated and quantitative assessment of aortic root based on cardiac computed tomography angiography using a new deep-learning tool: a comparison study

He Zou[1,2,3#], Yiqiu Jiang[1,2#], Haorui Huang[4], Ahmed Elkoumy[5,6], Xiaodong Wang[7], Jinyun Zhu[1,2], Youxian Shen[1,2], Xinmin Zhang[1,2], Mattia Lunadi[8], Osama Soliman[5], Lianpin Wu[1,2], Xinlei Wu[1,2]

[1]Zhejiang-Ireland Joint Laboratory for Precision Diagnosis and Treatment of Valvular Heart Diseases, The Second Affiliated Hospital of Wenzhou Medical University, Wenzhou, China; [2]Department of Cardiology, Key Laboratory of Panvascular Diseases of Wenzhou, School of the Second Clinical Medical Sciences, The Second Affiliated Hospital of Wenzhou Medical University, Wenzhou, China; [3]Department of Cardiology, The Wenzhou Third Clinical Institute Affiliated to Wenzhou Medical University, Wenzhou People's Hospital, Wenzhou, China; [4]School of the Biomedical Engineering, School of Ophthalmology and Optometry, Wenzhou Medical University, Wenzhou, China; [5]Saolta Group, Galway University Hospital, Health Service Executive and CORRIB Core Lab, University of Galway, Galway, Ireland; [6]Islamic Center of Cardiology, Al-Azhar University, Cairo, Egypt; [7]Research and Development Department, Suzhou Peixin Technology Co., Ltd., Suzhou, China; [8]Department of Cardiovascular Sciences, Fondazione Policlinico Universitario A. Gemelli IRCCS, Università Cattolica Sacro Cuore, Rome, Italy

Contributions: (I) Conception and design: L Wu, X Wu; (II) Administrative support: O Soliman, L Wu, X Wu; (III) Provision of study materials or patients: H Zou, Y Jiang, X Wu; (IV) Collection and assembly of data: H Huang, J Zhu, Y Shen, X Zhang; (V) Data analysis and interpretation: H Zou, A Elkoumy, X Wang, M Lunadi, X Wu; (VI) Manuscript writing: All authors; (VII) Final approval of manuscript: All authors.

[#]These authors contributed equally to this work.

Correspondence to: Xinlei Wu, PhD; Lianpin Wu, MD. Zhejiang-Ireland Joint Laboratory for Precision Diagnosis and Treatment of Valvular Heart Diseases, The Second Affiliated Hospital of Wenzhou Medical University, Jinlian Street, Innovation and Entrepreneurship Park, Wenzhou 325027, China; Department of Cardiology, Key Laboratory of Panvascular Diseases of Wenzhou, School of the Second Clinical Medical Sciences, The Second Affiliated Hospital of Wenzhou Medical University, Wenzhou, China. Email: xinlei.wu@wmu.edu.cn; 1187263152@qq.com.

Background: Accurate assessment of aortic root is crucial for the preprocedural planning of transcatheter aortic valve replacement (TAVR). A variety software is emerging for the semiautomated or automated measurements during TAVR planning. This study evaluated a new deep-learning (DL) tool based on cardiac computed tomography angiography (CCTA) for fully automatic assessment of aortic root.

Methods: The study included 126 patients with CCTA, 63 of whom underwent TAVR. In the overall population, the DL method was compared to manual measurements of the annulus dimensions. Within the TAVR group, the DL method was also compared to 3mensio software-derived aortic root measure, including the annulus, left ventricular outflow tract (LVOT), sinotubular junction (STJ), ascending aorta (AAo), and the heights of both the coronary ostia.

Results: Data were successfully analyzed using the DL method in 122 (96.8%) of patients. The correlation of annular diameters between the DL and manual methods was good to excellent for the overall cohort (n=118; r=0.83), the TAVR group (n=59, r=0.86), and its subgroups [bicuspid aortic valve (BAV): n=12, r=0.74; tricuspid aortic valve (TAV): n=47, r=0.93]. In the comparison of the DL method with 3mensio, the highest correlation was found for AAo (r=0.99). Among the four diameter indices [minimum, maximum, perimeter-derived diameter (pDD), and area-derived diameter (aDD)], excellent correlation was observed for aDD (LVOT: r=0.92; annulus: r=0.89).

Conclusions: The DL method offers an effective and efficient tool for the quantification of aortic roots for TAVR planning.

Keywords: Quantitative evaluation; cardiac computed tomography angiography (CCTA); deep-learning (DL)

Submitted Mar 30, 2024. Accepted for publication Sep 27, 2024. Published online Nov 11, 2024.
doi: 10.21037/qims-24-650
View this article at: https://dx.doi.org/10.21037/qims-24-650

Introduction

Transcatheter aortic valve replacement (TAVR) is widely acknowledged to be a safe and effective intervention for patients with severe aortic stenosis (AS) and is particularly well-suited for older adult patients (1,2). The application of TAVR is gradually expanding to encompass lower ages and low-risk populations (1,3) and even patients with aortic regurgitation (4,5). However, TAVR still presents potential complications, including coronary obstruction, paravalvular leakage, conduction disturbances, and annulus rupture (6-9). To optimize the procedure results and minimize the risk of complications, precise pre-TAVR assessment of the aortic root anatomy based on cardiac imaging is crucial for the optimal selection of the TAVR device in addition to the other procedural steps (3,10).

Multidetector spiral cardiac computed tomography angiography (CCTA) is the recommended imaging modality for evaluating aortic root anatomy due to its high spatial and temporal resolution (11,12). Based on the CCTA, quantitative analysis of the aortic annulus is, among others, the key assessment for determining the appropriate device size for TAVR (13). This method includes the measurement of the dimension of the aortic root, at the levels of the aortic annulus, left ventricular outflow tract (LVOT), sinuses of Valsalva (SOV), sinotubular junction (STJ), and the tubular tract of the ascending aorta (AAo), in addition to the assessment of calcification (14,15). Previous studies have examined the quantitative assessment of certain anatomic landmarks of aortic root using automatic detection methods based on CCTA images (16-18), and more recent advancements in automated and semiautomated algorithms or software have emerged to further improve the quantitative assessment of the aortic root (19-22). Meanwhile, manual measurement methods still relied on experienced experts, which is time-consuming and prone to reproducibility. Semiautomated software is considered an advancement due to its minimization of such limitations. More importantly, fully automated and rapid analysis of root structures is critical in the clinical scenario of emergency TAVR. However, clinical investigations for fully automatic measurement methods are scarce, especially in the Asian population with a high proportion of bicuspid aortic valve (BAV) and treated with TAVR (approximately 20–40%) (23).

Recently, a fully automatic deep-learning (DL) method, which was trained with the PyTorch framework (Meta AI, New York, NY, USA) was developed for the quantitative assessment of aortic root. This algorithm was integrated into the pre-TAVR measurement system (CardioVerse 1.0, Peixin Technology, Suzhou, China), which has received approval from the Government Medical Products Administration of Jiangsu Province. These advancements have been spurred by the growing use of new retrievable self-expanding devices with higher frames. In this study, we aimed to assess the feasibility and accuracy of this automatic DL tool from two main aspects. First, we assessed its feasibility and accuracy in measuring the aortic annulus by comparing it with highly experienced analysts using MIMICS software (Materialise, Leuven, Belgium). Second, we examined DL method in terms of the accuracy and consistency of quantitative measurements with more detailed parameters of aortic root in patients undergoing TAVR with self-expanding valves and compared them to those obtained using the widely employed 3mensio Structural Heart software (v. 10.3 SP1, Pie Medical Imaging, Maastricht, the Netherlands). We present this article in accordance with the GRRAS reporting checklist (available at https://qims.amegroups.com/article/view/10.21037/qims-24-650/rc).

Methods

Patient population and CCTA images

A retrospective validation was conducted involving 126 patients who underwent CCTA at The Second Affiliated Hospital of Wenzhou Medical University. The study population was categorized into two groups: a TAVR group (n=63), consisting of patients who underwent TAVR from March 2021 to August 2023, and a control group (n=63), consisting of patients with suspected cardiovascular disease (*Table 1*). *Figure 1* shows the flowchart of patient inclusion and group comparisons in this study.

Table 1 Clinical characteristics of the study population (n=118)

Category	Control group (n=59)	TAVR group (n=59)
Age (years), mean ± SD	71.1±9.1	76.2±8.1
Sex, n (%)		
Female	20 (33.9)	24 (40.7)
Male	39 (66.1)	35 (59.3)
Aortic valve disease, n (%)		
AS	–	55 (93.2)
AR	–	4 (6.8)
Aortic valve classification, n (%)		
TAV	59 (100.0)	47 (79.7)
BAV	0	12 (20.3)
Aortic annulus diameter, n (%)		
D ≤19 mm	1 (1.7)	0
19 mm < D ≤29 mm	57 (96.6)	56 (94.9)
29 mm < D	1 (1.7)	3 (5.1)
AAo mean diameter, n (%)		
AAo ≤40 mm	59 (100.0)	45 (76.3)
40 mm < AAo ≤50 mm	0	13 (22.0)
50 mm < AAo	0	1 (1.7)

TAVR, transcatheter aortic valve replacement; SD, standard deviation; AS, aortic valve stenosis; AR, aortic regurgitation; TAV, tricuspid aortic valve; BAV, bicuspid aortic valve (without raphe); D, diameter; AAo, ascending aorta.

All CCTA images were acquired using 256-slice multidetector systems with retrospective electrocardiogram (ECG) gating (SOMATOM Force, Siemens Healthineers, Erlangen, Germany; Brilliance iCT, Philips, Amsterdam, the Netherlands). Pixel spacing ranged from 0.33×0.33 to 0.68×0.68 mm^2, while slice thickness varied between 0.6 and 0.9 mm. Assessment of the CCTA images was conducted at the time point of best systole within the cardiac cycle. Aortic annulus was assessed with three methods (*Figure 2*), including manual annotation, the DL method, and 3mensio software. This study was conducted in accordance with the Declaration of Helsinki (as revised in 2013) and was approved by the Institutional Ethics Committee of The Second Affiliated Hospital of Wenzhou Medical University on November 28, 2022 (No. 2022-K-215-01). The requirement for individual consent was waived due to the retrospective nature of the analysis.

Aortic root assessment with a fully automatic algorithm

The algorithm of the DL method comprises three crucial steps for aortic root assessment: aortic root segmentation and centerline extraction, recognition of aortic valve classification, and multilevel localization and parameter measurement (Video S1). The average time for each automatic analysis was less than 2 minutes.

Aortic root segmentation and centerline extraction

To efficiently segment the aortic root complex of interest,

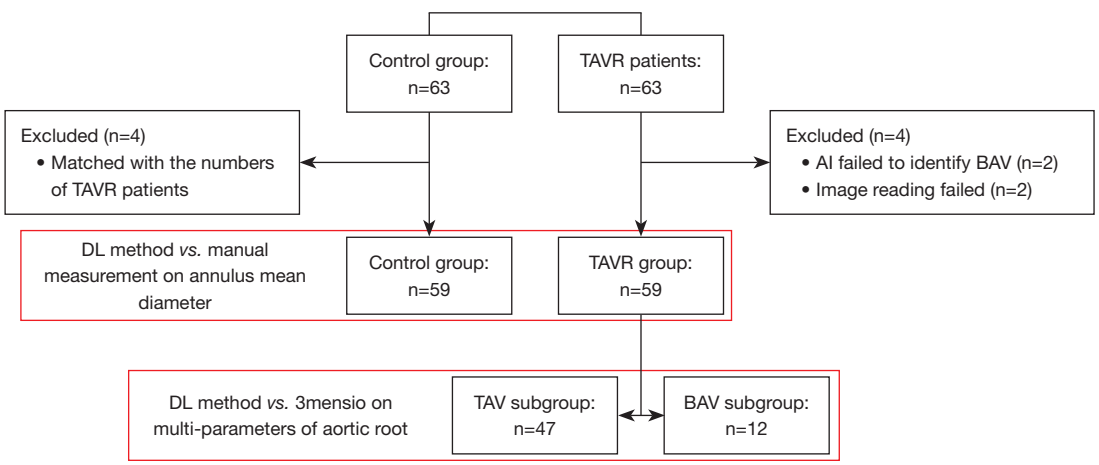

Figure 1 Schematic representation of patients included in this study. TAVR, transcatheter aortic valve replacement; AI, artificial intelligence; DL, deep learning; BAV, bicuspid aortic valve; TAV, tricuspid aortic valve.

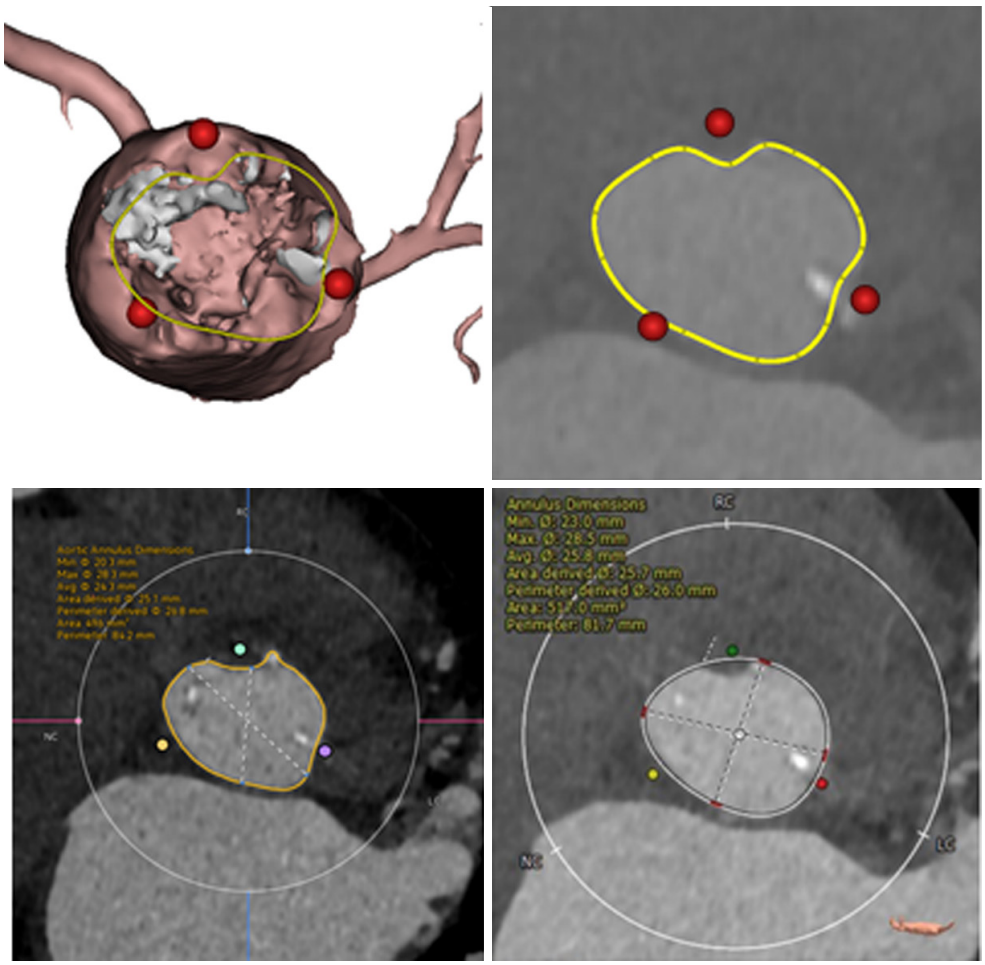

Figure 2 Three methods for assessing aortic annulus. The contour of aortic annulus identified by expert manual annotation on a 3D reconstructed aortic root model (top left) and reformatted image plane (top right) by the deep learning method (bottom left) and by 3mensio software (bottom right). The yellow and white curves around the aortic root means the contour identified by these methods.

including the AAo, LVOT, and coronary ostia, we employed the UNet++ DL model consisting of two networks (24). The first network was used to quickly identify the region of the aortic root complex by downsampling CCTA images with a coarse resolution. Subsequently, the centerline of the aortic root was extracted using a skeleton algorithm for the segmented mask of the aortic root and was followed by smoothing with a fifth-order Bessel curve.

Recognition of valve classification

With the identified aortic root region and centerline being used as inputs, the UNet++ model was then implemented with the second network at a high-resolution to further finely segment and subdivide the aortic root into specific components (i.e., AAo, LVOT, calcification, valve leaflets and coronary ostium). Tripartite structures (left, right, and noncoronary cusp) were trained for the DL method, and two classifications of the aortic valve [tricuspid aortic valve (TAV) and BAV] were recognized based on the numbers of coronary cusps (25). In our study, BAV was considered to be two cusps without fusion raphe, while TAV was considered to be three cusps including trileaflets with or without fusion raphe.

Multilevel localization and parameter measurement

According to expert consensus (2,10), the key levels of the aortic root complex were identified. First, the algorithm automatically located the SOV and determined the aortic valve phenotypes (TAV or BAV) based on the number of coronary cusps. For the BAV structure, a plane was

generated from the two lowest points of the sinuses and their orthogonality to a point on the centerline. The contour of the annular plane was determined using the shortest path of the center point to the aortic root. For the TAV structure, the annulus contour was identified with the three lowest points of the three sinuses (nadirs), which was determined by the morphological characteristics of the sinuses and their relationship with the centerline. Subsequently, the levels of LVOT and AAo were considered to be located 5 mm below and 40 mm above the annular plane, respectively, as these levels are commonly used for the high frame self-expanding valve in TAVR planning. The smoothed contour of these levels facilitated the calculation of indices such as minimum and maximum diameters, perimeter-derived diameter (pDD; calculated as length of cross-section contour/π), and the area-derived diameter (aDD; calculated as the square root of (4× area/π).

With the segmentation of the aorta and coronary arteries, the nearest distance algorithm was used to determine the intersection area between the left and right coronary artery orifices and the aorta. The heights of the left coronary ostium (LCH) and right coronary ostium (RCH) were determined through the following steps: Initially, local intersecting regions between the coronary ostia and the aorta were identified based on their morphologies following segmentation of the aorta and left and right coronary arteries; subsequently, the LCH and RCH were defined as the shortest Euclidean distances from the lower edges of these ostia to the annular plane, respectively.

Aortic root assessment by expert analysts

Manual measurements were conducted by a trained expert (Xinlei Wu) on all participants using MIMICS software (Materialise, Leuven, Belgium). The aortic root structure was segmented and reconstructed into a 3D model. The nadirs were identified in 2D slice CCTA images and simultaneously converted into a 3D model (*Figure 2*). Following this, a plane of the cross-section through these points was used as the basal plane to perform the multiplanar reformation of the CCTA images. Finally, the spline contour of the annulus was drawn on this reformatted image plane for calculating the mean diameter as: annulus contour length/π.

Aortic root assessment by 3mensio on TAVR patients

Aortic roots on the TAVR group were further assessed using 3mensio software (version 10.3, Pie Medical Imaging, Maastricht, the Netherlands) by a senior technician (Y.J.). To ensure accuracy, the assessments of two observers were cross-validated. Key parameters, including minimum, maximum, pDD, and aDD of the LVOT and aortic annulus, SOV, AAo, and both coronary ostial heights were recorded for comparison.

Statistical analysis

Categorical variables are presented as counts and percentages. Continuous data are presented as the mean ± standard deviation or as median with 25^{th} and 75^{th} percentiles, as appropriate. The normality distribution of the data was assessed with the Shapiro-Wilk test. The Mann-Whitney test was applied to determine if there were differences in annulus diameter between the DL and manual methods and between the non-TAVR and TAVR groups. For the aortic root assessment of the entire patient cohort, the differences in the mean diameter of the annulus plane between the DL method and expert manual measurement were evaluated with the *t*-test. The comparison of aortic root parameters within the TAVR group between the DL method and 3mensio software was analyzed with the *t*-test and Chi-squared test or with the Fisher exact test when the Cochran rule was not met. Bland-Altman plots were used to evaluate the error and bias between the DL method, expert manual measurement, and 3mensio software. The concordance correlation coefficient was analyzed as a measure of consistency between the DL method and the other methods. All statistical tests were two-sided, and a level of $P<0.05$ was considered statistically significant. All analyses were performed using Stata 12 (StataCorp, College Station, TX, USA).

Results

The assessment of aortic root was successfully executed by the fully automatic DL method in 122 of the 126 (96.8%) patients in the entire cohort, 64 (100%) patients in the non-TAVR group, and 59 (93.7%) patients in the TAVR group. The included patients in this study consisted of 59 patients (control group) with coronary artery disease and 59 patients with valvular heart disease who underwent TAVR. Distributions of the annulus diameter in deviation for the DL and manual methods for non-TAVR and TAVR groups were similar (Figure S1). The median annulus diameter deviation for the non-TAVR (–0.56 mm) and TAVR

Table 2 Comparison of key measurements of aortic root between the DL method and 3mensio in the TAVR group (n=59)

Index (mm)	DL method	3mensio	Difference	P value
LVOT				
Min D	20.1±3.7	20.5±3.4	−0.4±2.5	0.159
Max D	26.8 (24.4, 30.5)	28.3±4.2	−0.5 (−1.9, 1.0)	0.476
pDD	24.5 (22.1, 26.6)	25.0±3.7	−0.5 (−1.8, 0.9)	0.520
aDD	23.6 (21.5, 25.5)	23.8 (21.6, 26.1)	−0.4 (−1.6, 0.9)	0.576
Annulus				
Min D	20.9 (19.2, 22.9)	20.8±2.4	0.1 (−0.2, 0.4)	0.618
Max D	25.9 (24.0, 27.6)	26.0 (24.3, 28.2)	−0.4 (−1.3, 0.1)	0.275
pDD	23.7 (21.9, 25.1)	23.6 (22.1, 25.5)	0.2 (−0.6, 1.0)	0.640
aDD	23.2±2.7	23.4±2.2	−0.2±1.2	0.191
STJ, mean D	29.1±3.9	29.7±3.9	−0.6±1.0	<0.001
AAo, mean D	36.0±4.5	36.3±4.5	−0.3±0.5	<0.001
Coronary ostium height				
Left	12.1 (10.3, 14.7)	13.0 (11.1, 15.4)	−0.7 (−1.9, −0.4)	0.200
Right	17.1±3.2	15.4±2.7	1.7±2.8	<0.001

Data are reported as the mean ± standard deviation for normally distributed variables and as the median (25^{th}, 75^{th} percentiles) for nonnormally distributed variables. DL, deep learning; TAVR, transcatheter aortic valve replacement; LVOT, left ventricular outflow tract; D, diameter; pDD, perimeter-derived diameter; aDD, area-derived diameter; STJ, sinotubular junction; AAo, ascending aorta.

(−0.61 mm) groups was not significantly different (U=1,725; z=−0.083; P=0.934). The TAVR group comprised 47 patients with TAV and 12 patients with BAV.

Comparison of the DL method with manual measurement in all patients

The agreement and correlation between the DL method and expert manual measurement for the aortic annulus measurements are provided in Figure S2. The minimum value of the annular diameter difference between both methods was observed in the TAV subgroup (0.51±1.7 mm). The correlations for the mean diameter of aortic annulus between both methods were good for the overall patient cohort (r=0.83), the TAVR group (r=0.86), the TAV subgroup (r=0.87), and the BAV subgroup (r=0.74).

Comparison of the DL method with 3mensio software for the TAVR group

The aortic root parameter measurements obtained by the DL method were further compared with those derived from 3mensio software in the TAVR group (*Table 2*). No significant differences between the two methods were found for the four diameter indices of LVOT and annulus.

Figure 3 shows the Bland-Altman plots for the four indices of aortic annulus diameter in the TAVR group, indicating agreement between both methods, and scatterplots demonstrating the degree of correlation. An excellent correlation was observed between both methods for aDD of the annulus (r=0.89). Additionally, good correlations were found for the minimum, maximum, and pDD of the annulus (r=0.85, r=0.86, and r=0.87, respectively). The mean absolute differences for the annulus diameter indices were less than 0.4 mm. A similar observation was found for the four indices of LVOT, with good correlation (r=0.77, r=0.76, r=0.75, and r=0.92) between both measurements and all absolute differences were less than 0.5 mm, as shown in Figure S3.

The Bland-Altman plots and scatterplots comparing the DL method and 3mensio software measurements for STJ and AAo diameters, as well as for the LCH and RCH, are shown in Figure S4. The DL method and 3mensio software yielded significant differences for STJ and AAo diameters

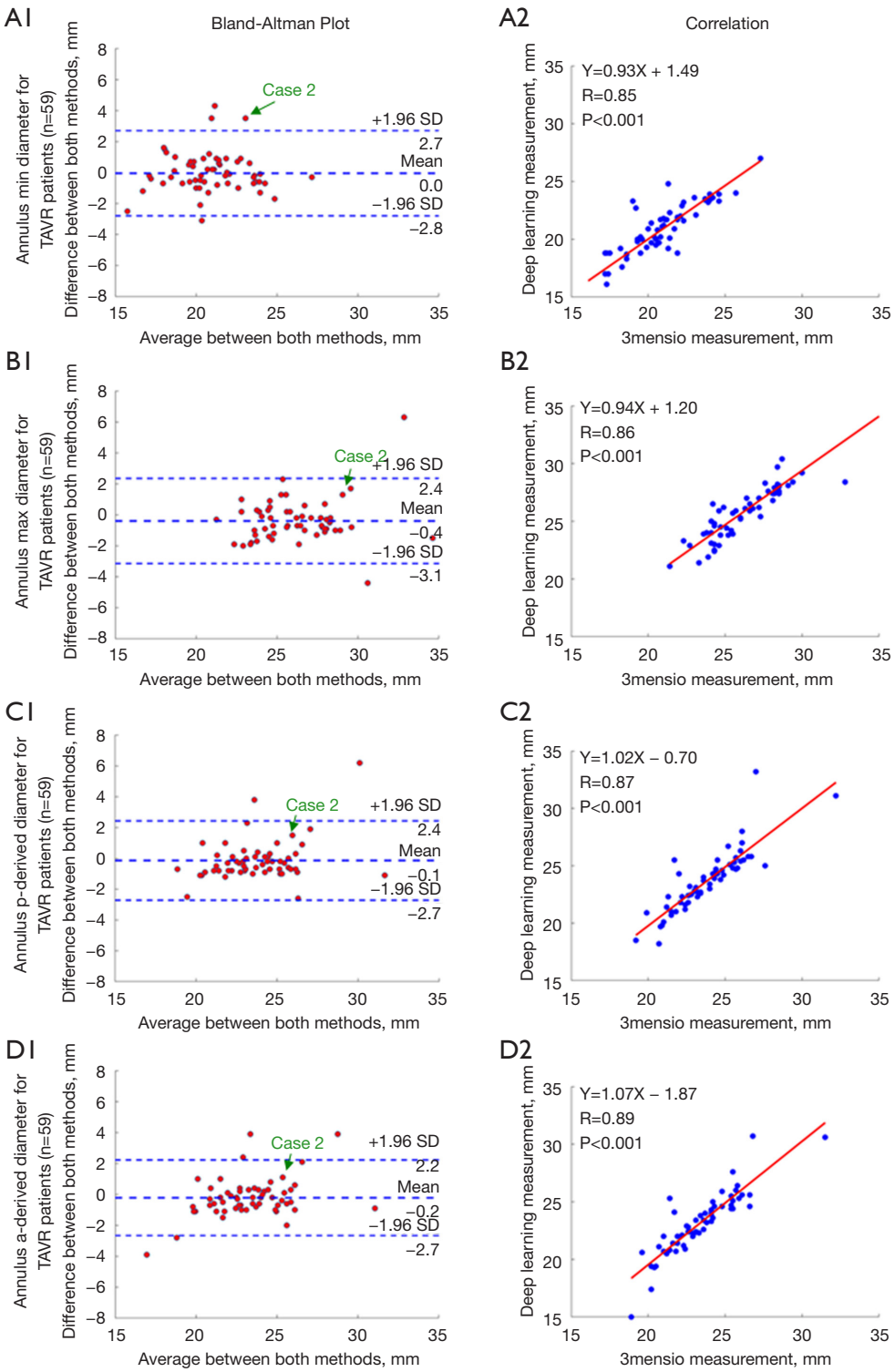

Figure 3 Bland-Altman plots and scatterplots of the new deep-learning method versus 3mensio software measurements for aortic annular minimum (A1,A2), maximum (B1,B2), perimeter-derived (C1,C2), and area-derived (D1,D2) diameter in the TAVR group. TAVR, transcatheter aortic valve replacement; p-derived, perimeter-derived; SD, standard deviation.

Table 3 Comparison of key measurements of aortic root between the DL method and 3mensio in the TAV subgroup (n=47)

Index (mm)	DL method	3mensio	Difference	P value
LVOT				
Min D	19.7±3.9	20.3±3.6	−0.5 (−1.3, 0.2)	0.162
Max D	26.4 (24.2, 30.4)	27.1 (25.3, 30.8)	−0.5 (−2.1, 1.1)	0.454
pDD	23.8 (21.9, 26.3)	24.8±3.9	−0.5 (−1.9, 1.1)	0.618
aDD	23.5±3.7	23.8±3.7	−0.4 (−0.8, 0.1)	0.095
Annulus				
Min D	20.7±2.7	20.7±2.4	0.0 (−0.4, 0.5)	0.872
Max D	25.7±2.5	25.5 (24.3, 28.2)	−0.4 (−1.4, 0.5)	0.302
pDD	23.4±2.4	23.4 (22.0, 25.5)	−0.2 (−1.0, 0.7)	0.658
aDD	23.0±2.6	23.1 (21.6, 25.3)	−0.2 (−1.1, 0.8)	0.739
STJ, mean D	28.6±3.8	29.1±3.7	−0.5±0.2	0.001
AAo, mean D	34.9±4.0	34.9±4.0	−0.3 (−0.5, −0.1)	<0.001
Coronary ostium height				
Left	11.8 (9.9, 15.1)	12.9 (10.5, 15.3)	−0.5 (−1.9, 0.7)	0.343
Right	16.5 (14.6, 19.7)	15.2±2.6	1.6 (0.5, 2.8)	0.009

Data are reported as the mean ± standard deviation for normally distributed variables and as the median (25^{th}, 75^{th} percentiles) for nonnormally distributed variables. DL, deep learning; TAV, tricuspid aortic valve; LVOT, left ventricular outflow tract; D, diameter; pDD, perimeter-derived diameter; aDD, area-derived diameter; STJ, sinotubular junction; AAo, ascending aorta.

(STJ: 29.1±3.9 *vs.* 29.7±3.9 mm, P<0.001; 36.0±4.5 *vs.* 36.3±4.5 mm, P<0.001), as well as for the RCH (17.1±3.2 *vs.* 15.4±2.7 mm; P<0.001). Moreover, their correlation was excellent, both for the STJ (r=0.97) and AAo (r=0.99). The LCH detected by DL method did not significantly differ from the 3mensio measurements (mean difference: 0.91mm; P=0.199), and there was a good correlation between both methods (r=0.71; P<0.001). However, the lowest concordance was found for the RCH (mean difference: −2.4 mm; r=0.52).

For the TAV subgroup, there was statistically similar deviations in these anatomic parameters (*Table 3*, Figures S5-S7). Excellent correlations were found for the four diameter indices of the annulus (r=0.83, r=0.91, r=0.90, and r=0.89, respectively) between both measurements with the small range of 1.96 standard deviations [(−3.0, 3.0), (−2.7, 1.6), (−2.3, 1.8), and (−2.7, 2.1); in Figure S5]. Excellent correlations were found for the aDD of LVOT (r=0.92) with a relatively small standard deviation, while the correlations of minimum, maximum, and pDD of LVOT were good (r=0.75, r=0.74, and r=0.73, respectively) with a larger range of 1.96 standard deviations [(−5.7, 4.6), (−7.3, 7.1), and (−6.7, 6.3), respectively; Figure S6]. Similarly, the correlations for the STJ (r=0.96) and AAo (r=0.99) were excellent (Figure S7). The lowest concordance was found for the RCH (mean difference −1.6 mm; concordance 0.51). The significant differences between both measurements were found for the STJ (28.6±3.8 *vs.* 29.1±3.7 mm; P<0.05), AAo (349±4.0 *vs.* 34.9±4.0 mm; P<0.001), and RCH [16.5 (14.6, 19.7) *vs.* 15.2±2.6 mm; P<0.05] but the absolute differences in these parameters were relatively small (STJ: −0.5 mm; AAo: −0.3 mm; LCH: −0.7 mm; RCH: 1.6 mm; Figure S7).

For the BAV subgroup, there were statistically similar deviations in these anatomic parameters (*Table 4*). Interestingly, the diameters of LVOT, STJ, and AAo for the BAV subgroup were significantly larger than those for the TAV subgroup. Excellent correlations were found for the four diameter indices of the annulus between both measurements (r=0.96, r=0.84, r=0.86, and r=0.91; Figure S8). The minimum diameter had the smallest range of 1.96 standard deviations, followed by aDD, pDD, and maximum diameter. The consistency and correlation of parameters for LVOT, STJ, AAo, LCH, and RCH in the

Table 4 Comparison key measurements of aortic root between the DL method and 3mensio in the BAV subgroup (n=12)

Index (mm)	DL method	3mensio	Difference	P value
LVOT				
Min D	21.3±3.0	21.4±2.5	−0.1±1.6	0.832
Max D	29.1±3.4	29.4±3.1	−0.3±1.5	0.529
pDD	25.6±2.9	26.2±2.7	−0.6±1.1	0.092
aDD	24.9±2.9	25.2±2.5	−0.4 (−1.0, 0.3)	0.235
Annulus				
Min D	21.1±2.1	21.4±2.3	−0.4±0.7	0.071
Max D	25.7 (25.1, 28.6)	26.8±1.9	−0.5 (−2.6, 1.7)	0.623
pDD	23.3 (22.9, 26.3)	24.2±1.8	−0.2 (−2.0, 2.0)	0.751
aDD	23.9±2.9	23.9±1.9	0.1±1.4	0.905
STJ, mean D	31.1±3.6	32.2±3.8	−1.2±0.8	<0.001
AAo, mean D	40.1±4.0	40.4±3.8	−0.3±0.4	0.034
Coronary ostium height				
Left	12.8 (11.3, 13.9)	14.7±3.7	−1.5 (−3.6, 0.7)	0.175
Right	18.4±3.2	16.2±1.5	2.2±2.8	0.020

Data are reported as the mean ± standard deviation for normally distributed and as the median (25^{th}, 75^{th} percentiles) for nonnormally distributed variables. DL, deep-learning; BAV, bicuspid aortic valve; LVOT, left ventricular outflow tract; D, diameter; pDD, perimeter-derived diameter; aDD, area-derived diameter; STJ, sinotubular junction; AAo, ascending aorta.

BAV subgroup are shown in Figures S9,S10.

Representative cases

Figure 4 illustrates several representative cases that exemplify the high concordance between the DL method and 3mensio measurements of aortic root indices. However, a large discrepancy was observed between the automatic DL tool and 3mensio measurements in some cases (*Figure 5*). A representative case of the large discrepancy in LVOT diameter was observed for case 1 (ΔDmax = −5.0 mm), where Δ is defined as follows: parameters derived by DL tool − parameters derived by 3mensio. Regarding the annulus measurements, a large difference was obtained for case 2 (ΔDmax =1.3 mm; *Figure 3*). Additionally, a large difference in LCH was observed for case 3 (ΔLCH = −15.0 mm). In this case, the anatomic variation of the location of the left coronary ostium caused large discrepancies between the methods. A large difference in RCH was also observed for case 4 (ΔRCH =−6.3 mm).

Discussion

The principal findings of this study can be summarized as follows: (I) the newly developed CCTA-based fully automatic DL method demonstrated feasibility and high accuracy in assessing aortic root in all enrolled patients. (II) The fully automatic quantification of aortic root measurements for patients treated with TAVR exhibited very good to excellent correlation measurements obtained using 3mensio—a commonly employed software for preprocedural planning.

Accurate modeling and quantitative analysis of the aortic root hold paramount importance for the correct sizing of percutaneous implantable aortic valve prostheses (26,27). As the gold standard imaging modality for pre-TAVR assessments, CCTA is the cornerstone for informing patient selection and planning treatment strategies (2,10). The development of a CCTA-based fully automatic DL method for discerning aortic root dimensions is urgently needed, especially given the diverse aortic anatomy and heightened prevalence of BAV observed in Asian patients

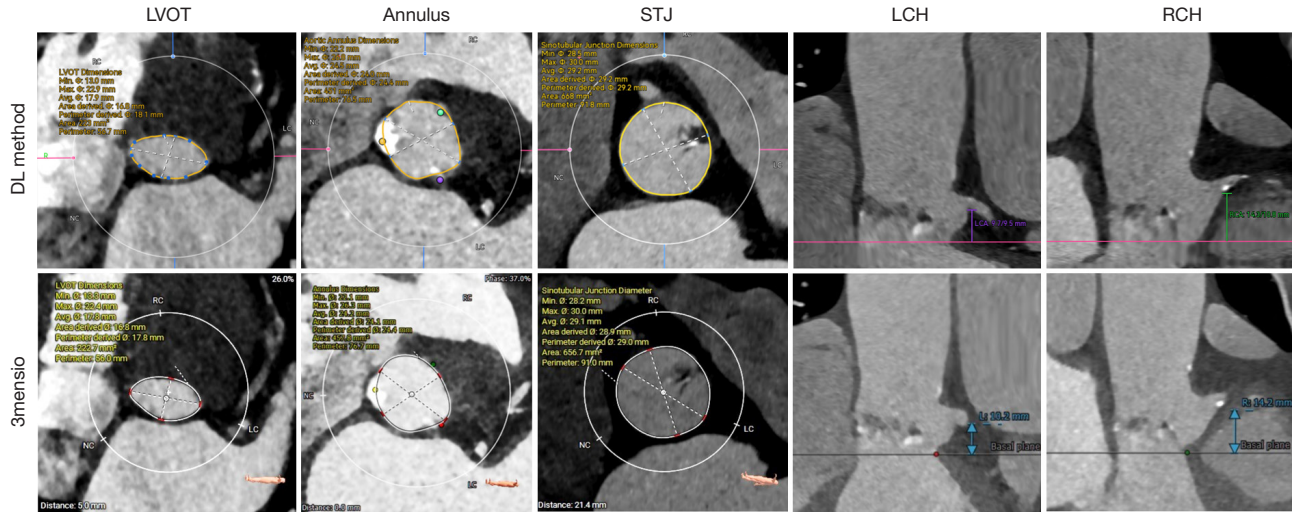

Figure 4 Comparison of deep learning method (top row) and 3mensio (bottom row) in key anatomical features in five representative cases with similar results. First to fifth column: LVOT, annulus, STJ, LCH, and RCH, respectively. The yellow (DL method) and white (3mensio) curves around the aortic root means the contour identified by these methods. LVOT, left ventricular outflow tract; STJ, sinotubular junction; LCH, height of left coronary ostium; RCH, height of right coronary ostium; DL, deep learning.

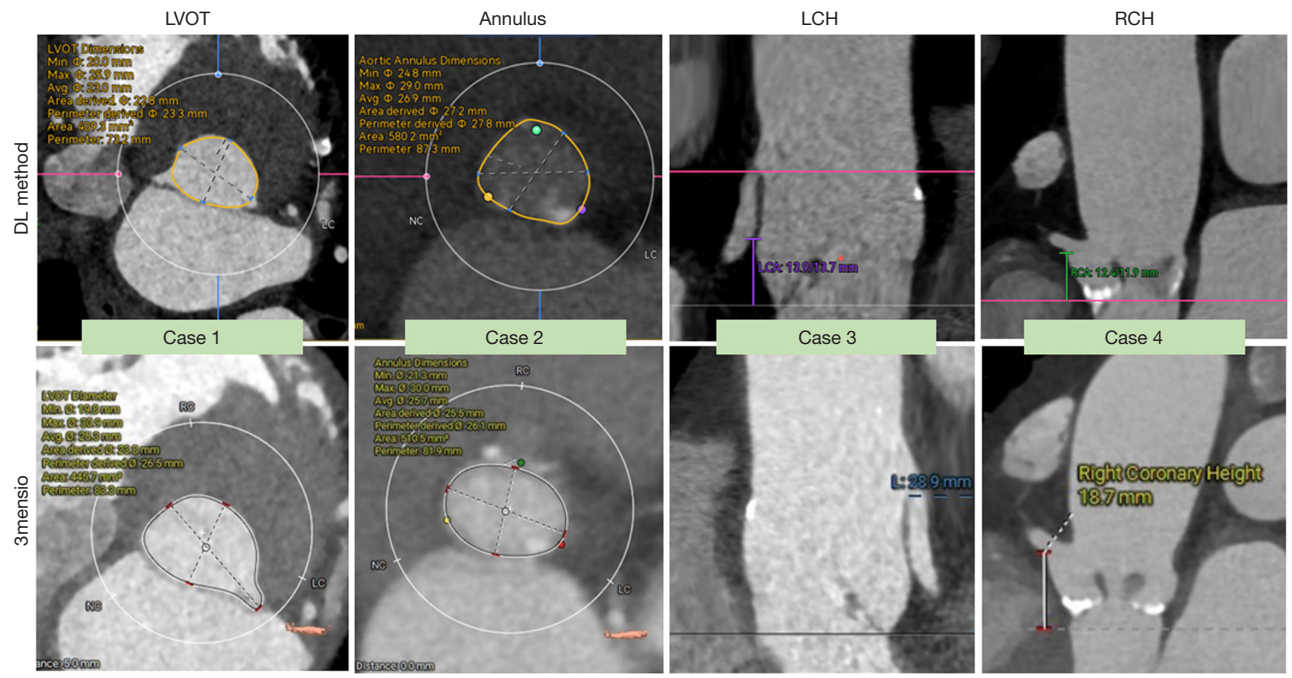

Figure 5 Comparison of the deep learning method (top row) and 3mensio (bottom row) in key anatomical features in five representative cases with significant differences. First to fourth column: LVOT, annulus, LCH, and RCH, respectively. The yellow (DL method) and white (3mensio) curves around the aortic root means the contour identified by these methods. LVOT, left ventricular outflow tract; LCH, height of left coronary ostium; RCH, height of right coronary ostium; DL, deep learning.

(23,28). In our study, the proposed DL method exhibited robust system performance and consistent accuracy across the entire patient cohort, which can be attributed to the machine learning training conducted on a sizable dataset encompassing over 500 pre-TAVR patient samples. Importantly, this algorithm demonstrated consistent efficacy even in real-world clinical scenarios, including cases characterized by substantial anatomical variations, pronounced artifacts, and poor imaging quality.

The mean difference between the DL method and expert manual measurement for the annulus mean diameter was less than 1 mm, except for the BAV subgroup. This could be acceptable for the selection of prosthesis with at least a 3-mm size gap based on the ratio of device-to-annulus. Given the inherently complex three-dimensional nature of the aortic annulus and LVOT (15), the four diameter indices, including the minimum, maximum, pDD, and aDD, obtained with the DL method were meticulously compared with those derived from 3mensio software. No statistically significant differences were discerned in these annulus-related indices or in LVOT between the DL method and 3mensio method across the TAVR, TAV, and BAV cohorts (*Tables 2-4*). aDD emerged as particularly noteworthy due to its superior correlation. This could be explained by the fact that aDD is derived from the contour area of cross-section, which could mitigate biases, especially in presence of irregular shapes.

Our findings underscore the necessity of a comprehensive evaluation in preprocedural assessments, which should include not only the subvalvular apparatus (annulus and LVOT) but also appropriate localization and assessment of the supravalvular structures (21,29). Not surprisingly, the minimum and maximum diameters of the aortic annulus and LVOT were significantly different, while the shapes of the STJ and AAo were circular. Our results are in line with previous reports (21,30). Notably, the automated DL measurements, although being notably smaller than those measured by 3mensio, showed relatively minor absolute differences (<1.2 mm) across all STJ and AAo levels. It is also worth mentioning that the absolute differences in these parameters were relatively small. Moreover, the RCH was significantly higher than the LCH. This divergence could be attributed to biases in annulus plane orientations or to the conversion of the distance of the aortic root curve into a straight-line distance from the annulus. Importantly, these marginal differences would not impact the selection of prosthetic size.

An additional advantage offered by this method is its fully automatic, one-stop solution, avoiding both interobserver and intraobserver variability in aortic root measurements. The application of the DL method can ensure a consistent and standardized approach, eliminating the potential biases introduced by manual interpretations. Importantly, the average duration of the analysis using the DL method was impressively efficient, at 1.8±2.0 minutes. This efficient performance was achieved on a general-purpose laptop equipped with an Intel Core i7 2.3-GHz processor boasting 16 cores, an NVIDIA GeForce RTX 3060 GPU, and 16 GB of memory. The duration depends upon the volume and quality of the CCTA images. In this study, our investigation revealed good-to-excellent correlation across all key levels of the aortic root for the TAVR group between the DL and 3mensio methods. The robust correlation observed across diverse patient profiles and aortic valve classifications underscores the efficiency and reliability of the proposed DL method in the context of pre-TAVR evaluations.

Although DL methods may be able to segment the anatomical structures with good precision, some features such as localized septal bulge or segmental septal hypertrophy (the funnel- or hourglass-shaped LVOT), presence of an abundant of calcium deposits, hypoattenuated leaflet thickening, anatomic variation of coronary ostium location, and poor image quality, could cause differences in diameters derived by the DL and 3mensio methods. Note that in one case, the poor image quality was caused by inadequate contrast agent perfusion with a low ejection fraction due to stress-induced cardiogenic shock after surgical femoral neck fracture treatment. Specifically, in patients with calcified lesions at the coronary ostium, insufficient segmentation precision may be more likely to cause errors of detection of the coronary ostium location, leading to substantial discrepancies in coronary ostium height. To address these challenges, a manual adjustment function is needed for correction in presence of an inappropriate deviation. Given the large number of cases tested by our DL method, it is reasonable to expect some large discrepancies in a few cases with respect to 3mensio measurements.

Limitations

Certain limitations to our study should be acknowledged. First, the automatic DL tool failed in a small subset of cases (4/126, 3.2%). Two cases involved incorrect classification of BAV as TAV, caused by the two nadir points of the

SOV being misidentified as three points. To address this, manual iterations could be integrated to modify nadir points, ensuring accurate classification of the aortic sinus, particularly in challenging anatomies such as type 0 BAV. The other two cases failed due to poor image quality and the large volume of image data with over 2,000 slides of whole-body scans. Large batches imported into the DL tool simultaneously can cause software crashes, and in this study, this was likely due to the high memory requirement for rendering the 3D model of the full body with the Graphical User Interface tool. Additionally, in real-world settings, especially with emergency patients who have extremely poor cardiac function, inadequate contrast perfusion during pre-procedural computed tomography (CT) angiography can lead to poor image quality, subsequently leading to failure of the software in identifying the nadirs of the sinus. Therefore, preselecting specific slide images of the aortic root complex is advisable for individual DL automatic analysis at a single time point. Second, our study exclusively concentrated on the comparison of quantitative parameters measured by the fully automatic DL method for aortic root assessment and did not incorporate the segmentation of calcium deposits. The distribution and extent of calcium deposits play a pivotal role in tailoring patient-specific oversizing and downsizing strategies in selecting the appropriate TAVR device size (6,31). The challenges associated with training a calcium segment model are influenced by several factors, such as CT equipment, calcium density, and threshold values on CT images. A potential solution lies in integrating a segment function with manual interaction, allowing for the setting of variable thresholds to facilitate the fast segmentation of calcified masses. Third, our investigation constituted a moderately sized single-center study, incorporating retrospectively enrolled patients. The patient cohort were exclusively from the southeastern China, and thus the potential influence of morphological variations associated with racial diversity might have been overlooked, limiting the generalizability of the DL method. Consequently, validation in a larger, prospective, and global multicenter study is imperative to establish the robustness of this novel method across diverse populations. Finally, while our study demonstrated a commendable correlation in aortic root assessment between the DL method and other methods, its application in clinical practice for guiding treatment strategies in minimizing complications necessitates further validation through a clinical, prospective study conducted across multiple centers. Owing to its speed, the new DL method may be well-suited to performing analysis of large populations. Additionally, it may allow for accurate and individualized TAVR planning and may thus improve outcomes.

Conclusions

The proposed DL algorithm achieved accurate identification and measurement of aortic root dimensions based on CCTA and demonstrated high feasibility. The fully automated and rapid quantification offered by the DL method can facilitate efficient and objective preprocedural assessment, especially for patients requiring emergency TAVR.

Acknowledgments

Funding: This research was supported by the Zhejiang Provincial Natural Science Foundation of China (No. LTGY24H180019 to Xinlei Wu), the Medical and Health Science and Technology Project of Zhejiang Province (Nos. 2023RC210 and 2024KY160 to Xinlei Wu), and the Jie Bang Gua Shuai Project of Wenzhou Science and Technology Bureau (No. ZY2023022 to L.W. and No. ZY2024019 to Xinlei Wu).

Footnote

Reporting Checklist: The authors have completed the GRRAS reporting checklist. Available at https://qims.amegroups.com/article/view/10.21037/qims-24-650/rc

Conflicts of Interest: All authors have completed the ICMJE uniform disclosure form (available at https://qims.amegroups.com/article/view/10.21037/qims-24-650/coif). Xinlei Wu received funding from the Zhejiang Provincial Natural Science Foundation of China (No. LTGY24H180019) and the Medical and Health Science and Technology Project of Zhejiang Province (Nos. 2023RC210 and 2024KY160). L.W. received funding from the Jie Bang Gua Shuai Project of Wenzhou Science and Technology Bureau (No. ZY2023022). Xiaodong Wang is the CEO of Peixin Technology Co., Ltd. The other authors have no conflicts of interest to declare.

Ethical Statement: The authors are accountable for all aspects of the work in ensuring that questions related to the accuracy or integrity of any part of the work are

appropriately investigated and resolved. This study was conducted in accordance with the Declaration of Helsinki (as revised in 2013) and was approved by the Institutional Ethics Committee of The Second Affiliated Hospital of Wenzhou Medical University on November 28, 2022 (No. 2022-K-215-01). The requirement for individual consent was waived due to the retrospective nature of the analysis.

References

1. Leon MB, Smith CR, Mack MJ, Makkar RR, Svensson LG, Kodali SK, et al. Transcatheter or Surgical Aortic-Valve Replacement in Intermediate-Risk Patients. N Engl J Med 2016;374:1609-20.
2. Otto CM, Nishimura RA, Bonow RO, Carabello BA, Erwin JP 3rd, Gentile F, Jneid H, Krieger EV, Mack M, McLeod C, O'Gara PT, Rigolin VH, Sundt TM 3rd, Thompson A, Toly C. 2020 ACC/AHA Guideline for the Management of Patients With Valvular Heart Disease: A Report of the American College of Cardiology/American Heart Association Joint Committee on Clinical Practice Guidelines. J Am Coll Cardiol 2021;77:e25-e197.
3. Yerasi C, Rogers T, Forrestal BJ, Case BC, Khan JM, Ben-Dor I, Satler LF, Garcia-Garcia HM, Cohen JE, Kitahara H, Shults C, Waksman R. Transcatheter Versus Surgical Aortic Valve Replacement in Young, Low-Risk Patients With Severe Aortic Stenosis. JACC Cardiovasc Interv 2021;14:1169-80.
4. Liu R, Fu Z, Jiang Z, Yan Y, Yao J, Liu X, Yan X, Song G. Transcatheter aortic valve replacement for aortic regurgitation: a systematic review and meta-analysis. ESC Heart Fail 2024. [Epub ahead of print]. doi: 10.1002/ehf2.14832.
5. Poletti E, De Backer O, Scotti A, Costa G, Bruno F, Fiorina C, et al. Transcatheter Aortic Valve Replacement for Pure Native Aortic Valve Regurgitation: The PANTHEON International Project. JACC Cardiovasc Interv 2023;16:1974-85.
6. Abdelkhalek M, Daeian M, Keshavarz-Motamed Z. Regional assessment of aortic valve calcification using topographic maps in contrast-enhanced CT: in-vivo sex and severity-based differences in calcific presentation. Quant Imaging Med Surg 2024;14:1-19.
7. Khan JM, Kamioka N, Lisko JC, Perdoncin E, Zhang C, Maini A, et al. Coronary Obstruction From TAVR in Native Aortic Stenosis: Development and Validation of Multivariate Prediction Model. JACC Cardiovasc Interv 2023;16:415-25.
8. Tang GHL, Zaid S. Commissural (Mis)Alignment in TAVR and Hemodynamic Impact: More Questions Raised Than Answered. JACC Cardiovasc Interv 2022;15:1137-9.
9. Wiktorowicz A, Wit A, Malinowski KP, Dziewierz A, Rzeszutko L, Dudek D, Kleczynski P. Paravalvular leak prediction after transcatheter aortic valve replacement with self-expandable prosthesis based on quantitative aortic calcification analysis. Quant Imaging Med Surg 2021;11:652-64.
10. Vahanian A, Beyersdorf F, Praz F, Milojevic M, Baldus S, Bauersachs J, et al. 2021 ESC/EACTS Guidelines for the management of valvular heart disease. Eur J Cardiothorac Surg 2021;60:727-800.
11. Blanke P, Weir-McCall JR, Achenbach S, Delgado V, Hausleiter J, Jilaihawi H, Marwan M, Nørgaard BL, Piazza N, Schoenhagen P, Leipsic JA. Computed Tomography Imaging in the Context of Transcatheter Aortic Valve Implantation (TAVI)/Transcatheter Aortic Valve Replacement (TAVR): An Expert Consensus Document of the Society of Cardiovascular Computed Tomography. JACC Cardiovasc Imaging 2019;12:1-24.
12. Francone M, Budde RPJ, Bremerich J, Dacher JN, Loewe C, Wolf F, Natale L, Pontone G, Redheuil A, Vliegenthart R, Nikolaou K, Gutberlet M, Salgado R. CT and MR imaging prior to transcatheter aortic valve implantation: standardisation of scanning protocols, measurements and reporting-a consensus document by the European Society of Cardiovascular Radiology (ESCR). Eur Radiol 2020;30:2627-50. Erratum in: Eur Radiol 2020;30:4143-4.
13. Wu X, Serruys PW, Wu T, Ruan Z, Xue W, Wu D, Wu L, Zhang X. TCTAP A-105 A New Method of Prosthesis Virtual Implantation for Pre-Procedural Assessment of TAVR: Comparison of Self-Expandable Devices in a Patient With Bicuspid Aortic Valve With Severe Stenosis and Calcification. J Am Coll Cardiol 2023;81:S69-S70.

14. Stortecky S, Heg D, Gloekler S, Wenaweser P, Windecker S, Buellesfeld L. Accuracy and reproducibility of aortic annulus sizing using a dedicated three-dimensional computed tomography reconstruction tool in patients evaluated for transcatheter aortic valve replacement. EuroIntervention 2014;10:339-46.
15. Messika-Zeitoun D, Serfaty JM, Brochet E, Ducrocq G, Lepage L, Detaint D, Hyafil F, Himbert D, Pasi N, Laissy JP, Iung B, Vahanian A. Multimodal assessment of the aortic annulus diameter: implications for transcatheter aortic valve implantation. J Am Coll Cardiol 2010;55:186-94.
16. Watanabe Y, Morice MC, Bouvier E, Leong T, Hayashida K, Lefèvre T, Hovasse T, Romano M, Chevalier B, Donzeau-Gouge P, Farge A, Cormier B, Garot P. Automated 3-dimensional aortic annular assessment by multidetector computed tomography in transcatheter aortic valve implantation. JACC Cardiovasc Interv 2013;6:955-64.
17. Murphy DT, Blanke P, Alaamri S, Naoum C, Rubinshtein R, Pache G, Precious B, Berger A, Raju R, Dvir D, Wood DA, Webb J, Leipsic JA. Dynamism of the aortic annulus: Effect of diastolic versus systolic CT annular measurements on device selection in transcatheter aortic valve replacement (TAVR). J Cardiovasc Comput Tomogr 2016;10:37-43.
18. Astudillo P, Mortier P, Bosmans J, De Backer O, de Jaegere P, Iannaccone F, De Beule M, Dambre J. Automatic Detection of the Aortic Annular Plane and Coronary Ostia from Multidetector Computed Tomography. J Interv Cardiol 2020;2020:9843275.
19. Gumsheimer M, Stortecky S, Gahl B, Langhammer B, Carrel T, Buellesfeld L, Huber C, Most H. Validation of 3D-reconstructed computed tomography images using OsiriX® software for pre-transcatheter aortic valve implantation aortic annulus sizing. Interact Cardiovasc Thorac Surg 2017;25:198-205.
20. Saitta S, Sturla F, Gorla R, Oliva OA, Votta E, Bedogni F, Redaelli A. A CT-based deep learning system for automatic assessment of aortic root morphology for TAVI planning. Comput Biol Med 2023;163:107147.
21. Wang M, Niu G, Chen Y, Zhou Z, Feng D, Zhang Y, Wu Y; China-DVD2 Study Group (Standard Evaluation and Optimal Treatment for Elderly Patients with Valvular Heart Disease, National Key R&D Program of China, NCT05044338). Development and validation of a deep learning-based fully automated algorithm for pre-TAVR CT assessment of the aortic valvular complex and detection of anatomical risk factors: a retrospective, multicentre study. EBioMedicine 2023;96:104794.
22. Baeßler B, Mauri V, Bunck AC, Pinto Dos Santos D, Friedrichs K, Maintz D, Rudolph T. Software-automated multidetector computed tomography-based prosthesis-sizing in transcatheter aortic valve replacement: Inter-vendor comparison and relation to patient outcome. Int J Cardiol 2018;272:267-72.
23. Yang LT, Lo HY, Lee CC, Takeuchi M, Hsu TC, Tsai CM, Michelena HI, Enriquez-Sarano M, Chen YS, Chen WJ, Ho YL. Comparison Between Bicuspid and Tricuspid Aortic Regurgitation: Presentation, Survival, and Aorta Complications. JACC Asia 2022;2:476-86.
24. Zhou Z, Siddiquee MMR, Tajbakhsh N, Liang J. UNet++: Redesigning Skip Connections to Exploit Multiscale Features in Image Segmentation. IEEE Trans Med Imaging 2020;39:1856-67.
25. Jilaihawi H, Chen M, Webb J, Himbert D, Ruiz CE, Rodés-Cabau J, et al. A Bicuspid Aortic Valve Imaging Classification for the TAVR Era. JACC Cardiovasc Imaging 2016;9:1145-58.
26. Prihadi EA, van Rosendael PJ, Vollema EM, Bax JJ, Delgado V, Ajmone Marsan N. Feasibility, Accuracy, and Reproducibility of Aortic Annular and Root Sizing for Transcatheter Aortic Valve Replacement Using Novel Automated Three-Dimensional Echocardiographic Software: Comparison with Multi-Detector Row Computed Tomography. J Am Soc Echocardiogr 2018;31:505-514.e3.
27. Wu X, Serruys PW, Yu X, Sun Y, Chen Y, Wu D, Zhang X, Wu L. TCTAP C-201 Optimal Implantation Depth of a Self-Expandable TAVR Device in a Patient With Type 0 Bicuspid Aortic Valve With Severe Stenosis and Calcification Guided by In-Silico Simulation. J Am Coll Cardiol 2023;81:S434-S435.
28. Liu X, He Y, Zhu Q, Gao F, He W, Yu L, Zhou Q, Kong M, Wang J. Supra-annular structure assessment for self-expanding transcatheter heart valve size selection in patients with bicuspid aortic valve. Catheter Cardiovasc Interv 2018;91:986-94.
29. Zhang X, Wu H, Pan Z, Elkoumy A, Ruan Z, Wu T, Wu D, Soliman O, Wu L, Wu X. Mechanism of balloon burst during transcatheter aortic valve replacement pre-dilatation: Image observation and validation by finite element analysis. Comput Biol Med 2024;168:107714.
30. Theriault-Lauzier P, Alsosaimi H, Mousavi N, Buithieu J, Spaziano M, Martucci G, Brophy J, Piazza N. Recursive multiresolution convolutional neural networks for 3D

aortic valve annulus planimetry. Int J Comput Assist Radiol Surg 2020;15:577-88.
31. Yeats BB, Sivakumar SK, Samaee M, Polsani V, Yadav PK, Thourani VH, Sellers S, Sathananthan J, Dasi LP. Calcium Fracture and Device Over Expansion in Transcatheter Aortic Valve Replacement for Bicuspid Aortic Valves. Ann Biomed Eng 2023;51:2172-81.

Cite this article as: Zou H, Jiang Y, Huang H, Elkoumy A, Wang X, Zhu J, Shen Y, Zhang X, Lunadi M, Soliman O, Wu L, Wu X. Automated and quantitative assessment of aortic root based on cardiac computed tomography angiography using a new deep-learning tool: a comparison study. Quant Imaging Med Surg 2024;14(12):8414-8428. doi: 10.21037/qims-24-650